



# Quantitative determination by temperature dependent near-infrared spectra

Xueguang Shao\*, Jun Kang, Wensheng Cai

Research Center for Analytical Sciences, College of Chemistry, Nankai University, Tianjin 300071, PR China

## ARTICLE INFO

### Article history:

Received 8 April 2010

Received in revised form 2 June 2010

Accepted 2 June 2010

Available online 11 June 2010

### Keywords:

Near-infrared spectroscopy

Temperature

Quantitative determination

Quantitative spectra–temperature

relationship

Partial least squares regression

## ABSTRACT

Near-infrared (NIR) spectra are sensitive to the variation of experimental conditions, such as temperature. In this work, the relationship between NIR absorption spectra and temperature was quantitatively analyzed and applied to the quantitative determination of the compositions in mixtures. It was found that, for the solvents such as water and ethanol, a quantitative spectra–temperature relationship (QSTR) model between NIR spectra and temperature can be established by using partial least squares (PLS) regression. Therefore, the temperature of a solution can be predicted by using the model and NIR spectrum. Furthermore, it was also found that the difference between the predicted results of different solutions is a quantitative reflection of concentration. The variation of intercept in the relationship of the predicted and measured temperature can be used to determine the concentration of the compositions. The mixtures of water, methanol, ethanol and ethylenediamine in a concentration range of 5–80% (v/v) were studied. The calibration curves are found to be reliable with the correlation coefficients ( $R$ ) higher than 0.99. Both the QSTR and calibration model may extend the application of NIR spectroscopy and provide novel techniques for analytical chemistry.

© 2010 Elsevier B.V. All rights reserved.

## 1. Introduction

Near-infrared (NIR) spectra, as a kind of vibrational spectra, show not only isolated molecular features such as structure and functional groups but also inter- or intra-molecular features including hydrogen bonding. The variation of temperature will bring the changes in both inter- and intra-molecular interactions [1–3], and therefore the NIR spectra detected under different temperature can reflect these changes. This may provide new ways for structural and process analyses.

The effects of temperature on NIR spectrum of water were reported as early as in 1925 [4]. The temperature dependence of the absorption spectrum of liquid water in the range of 700–2100 nm from 0 to 95 °C was studied. In the further studies, works over similar spectral region were continued covering a large range of temperature (0–372.5 °C) [5,6]. Three decades later, works were followed by a number of groups in different aspects. It was observed that the maximum of the absorption band at 1450 nm varies with temperature and the variation is attributed to the change of the H-bond strength [7]. On the other hand, the absorptivity temperature coefficients as a function of wavelength from 550 to 900 nm for liquid water over the range 15–60 °C were reported [8], and liquid D<sub>2</sub>O [9], water-adsorbed starch and cellulose [10], glucose solutions [11], *N*-methylacetamide–water complexes [12], alco-

hol/water binary mixtures [3,13] and polyamide [14,15] were also investigated. Furthermore, applications of temperature dependent NIR spectra have been well reported, e.g., the dissociation and thermodynamic properties of *N*-methylacetamide [16] and identification of the existence of two species in water [17]. Temperature dependent spectra have been a way to generate two-dimensional (2D) mid infrared (IR) and NIR correlation spectroscopy that has been widely used in spectroscopic studies [2,3,13–16,18–20].

Chemometric methods were extensively applied to the studies of temperature dependent NIR spectra [17,21–24], because multivariate analysis must be adopted. The influence of the temperature-induced spectral variations on the predictive ability of multivariate calibration models was studied [25,26]. Efforts to correct the effect of temperature variation on NIR spectra were made because it was known as a perturbation that affects NIR spectra and the predictive ability of multivariate models. Piecewise direct standardization (PDS), which is used for correction of the nonlinear spectral effects, was developed to standardize the spectra at different temperatures [27], and a temperature correction method for the monitoring of a polymorph conversion process was proposed [28]. Furthermore, temperature-insensitive calibration methods based on chemometric strategies [29–31] were studied and applied to the measurement of protein concentration in aqueous solutions by near-infrared spectroscopy [32,33]. On the other hand, rather than seeing the spectroscopic temperature effects as artefacts that have to be circumvented or eliminated, temperature was also introduced to generate three-way dataset for multivariate spectroscopic analysis [34].

\* Corresponding author. Tel.: +86 22 23503430; fax: +86 22 23502458.  
E-mail address: [xshao@nankai.edu.cn](mailto:xshao@nankai.edu.cn) (X. Shao).

In this paper, effects of temperature on NIR spectra are considered as useful information, from which quantitative models are established by using partial least squares (PLS) regression. The temperature dependent NIR spectra of commonly used solvents (water, methanol, ethanol, *n*-hexane) and their mixtures with ethylenediamine are studied. The quantitative spectra–temperature relationship (QSTR) model between NIR spectra and temperature are studied. Results show that the temperature of a solution can be quantitatively predicted by using the model and NIR spectrum. In addition, the difference between the predicted results of different solutions is found to be a quantitative reflection of concentration. Quantitative calibration curves for concentration are established with the intercepts in the relationship of the predicted and measured temperature.

## 2. Experimental

### 2.1. Reagents

All reagents, including methanol, ethanol, *n*-hexane and ethylenediamine, were of analytical grade. Purified water, provided by Wahaha Company (Hangzhou, China), was used throughout.

### 2.2. Sample preparation

Two groups of samples were prepared for this study. The first group was used for investigation of the relationship between temperature and spectra. Water, methanol, ethanol, *n*-hexane and ethylenediamine were used, and a series of mixtures were prepared, including water–ethanol (50:50, v/v), ethanol–*n*-hexane (50:50, v/v), water–ethylenediamine (50:50, v/v), ethanol–ethylenediamine (50:50, v/v), water–methanol–ethanol (50:25:25, v/v/v) and water–ethanol–ethylenediamine (25:25:50, v/v/v). The second group was used for investigation of calibration curves. Binary and three-component solutions were prepared as listed in Table 1.

In order to validate the calibration curve for ethanol, two aqueous ethanol solutions (10%, 70%, v/v) and a Chinese alcohol liquor sample were adopted. The alcohol liquor sample was used without any pretreatment.

### 2.3. Measurement of temperature and spectrum

A three-necked flask containing 100 mL samples was placed in an oil-bath system (Yuhua, Gongyi, China) comprising of a temperature control unit and magnetic stirrer. The stability of the system for temperature control is  $\pm 1^\circ\text{C}$ , but the temperature was measured with a thermometer plugged into the flask. The temperature was controlled to change from 25 to 60  $^\circ\text{C}$  with a step of ca. 3  $^\circ\text{C}$ . The spectrum at each temperature was measured 20 min later when the temperature was changed.

All NIR spectra were measured from 5500 to 12,000  $\text{cm}^{-1}$  by a Vertex 70 spectrometer (Bruker Optics Inc., Ettlingen, Germany) furnished with a transmittance optical fiber probe (Bruker Optics Inc., Ettlingen, Germany) of optical path 2 mm. A tungsten-halogen light source and InGaAs detector were used. The spectra are digitalized with ca. 4  $\text{cm}^{-1}$  interval in the Fourier transform, each

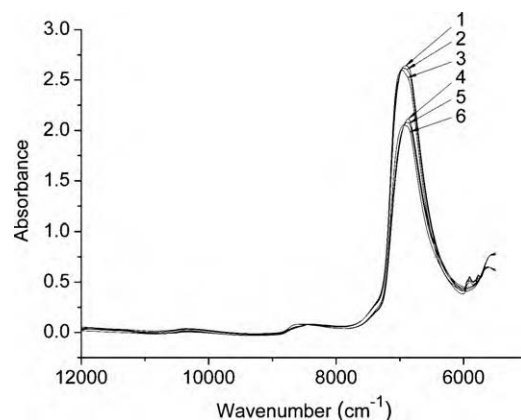


Fig. 1. NIR spectra of water (1, 2 and 3) and 30% aqueous ethanol solution (4, 5 and 6) at 32, 38 and 50  $^\circ\text{C}$ .

spectrum is, therefore, composed of 1686 data points. To increase signal to noise ratio, both air reference and sample spectra were measured with scan number 64.

As examples, Fig. 1 shows the measured NIR spectra of pure water and 30% aqueous ethanol solution under three different temperatures. It can be seen that there is only very small difference between the spectra of different temperatures. Even for the spectra of pure water and aqueous ethanol solution, there is only the difference in the peak intensity, whereas no obvious change in the shape. It is difficult to find quantitative relationship directly from the spectra. Therefore, multivariate calibration was used in this study.

### 2.4. PLS modeling

PLS regression method was used for modeling and prediction, and all calculations were carried out in Matlab (Math Works, Inc., Natick, MA). The performance of PLS regression models was evaluated in terms of the correlation coefficient ( $R$ ) and the root mean square error of cross validation (RMSECV), which was determined by leave-one-out cross validation (LOO-CV). The number of latent variables for PLS model was determined by using the LOO-CV with  $F$ -test [35]. Furthermore, due to the drifting baseline or background in the spectra, continuous wavelet transform for approximate derivative (CWTAD) technique was used for spectral pre-processing.

## 3. Results and discussion

### 3.1. Quantitative spectra–temperature relationship

Although the effects of temperature on the NIR spectra have been well studied, it is hard to explain the details directly from the inspection of the spectral changes, e.g., for the cases shown in Fig. 1. In order to study the quantitative relationship between NIR spectra and temperature, PLS regression was used, and LOO-CV was employed for evaluation of the PLS model.

Fig. 2 shows the relationship between the predicted and measured temperature of pure water, and the result of cross validation is listed in the first line of Table 2. In the calculation, 12 measured data for the temperature from 24 to 60  $^\circ\text{C}$  were used, and four was used as the number of latent variables for the PLS model. Clearly, the figure shows a very good linearity between the predicted and measured temperature. The correlation coefficient ( $R$ ) is as high as 0.9998, and the root mean square error of cross validation (RMSECV) is only 0.1739. This result indicates that a QSTR model do exist to describe the relationship between temperature

Table 1  
Compositions of the prepared samples.

Solvent	Solute	Concentration (% v/v)
Water	Ethanol	5, 20, 30, 50, 60, 80
Ethanol	Ethylenediamine	10, 20, 30, 50, 70, 80
Water–ethanol (1:1, v/v)	Ethylenediamine	10, 20, 30, 50, 70, 80
Water	Ethanol (25% methanol)	5, 10, 20, 30, 50, 70

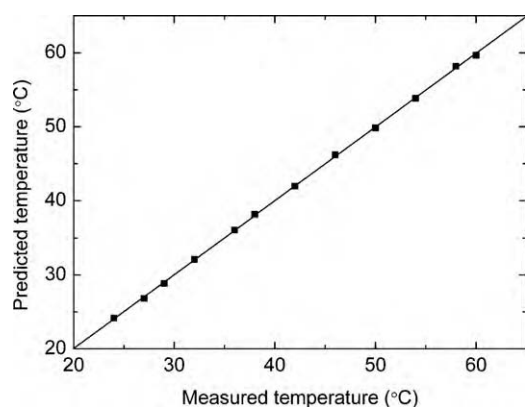


Fig. 2. Relationship of the measured and predicted temperature of water over the temperature range 24–60 °C.

and NIR spectra, and it can be modeled by PLS regression. Furthermore, the same experiments and calculations were also performed for ethanol and *n*-hexane, respectively. Results obtained are summarized in Table 2, line 2 and 3. It can be seen that the quality of the QSTR models is almost the same as that of the pure water.

For further investigation of the QSTR model, NIR spectra of two- and three-component mixtures of water–ethanol, ethanol–*n*-hexane, water–ethylenediamine, ethanol–ethylenediamine, water–methanol–ethanol and water–ethanol–ethylenediamine were measured under different temperature. The results of cross validation are displayed in Table 2 from line 4 to 9. From the table, it can be concluded that the QSTR model between temperature and NIR spectra is also valid for two- and three-component mixtures. Furthermore, the results also indicate that, not only the solvents like water and ethanol that contain O–H bond can be modeled by the method, mixtures of compounds that contain N–H bond also have the same behavior.

On the other hand, it is worthy of note that all the measured data (1686 variables) of the spectra from 5500 to 12,000  $\text{cm}^{-1}$  were used in the calculations above. In fact, there is much redundant information by using all the variables. Thus, the models built with different wavelength bands were investigated. Inspiringly, it was found that models with the same quality as listed in Table 2 can be obtained by using only a small part, e.g., 100, of the variables in the wavelength range from 5500 to 10,000  $\text{cm}^{-1}$ . If the variables in the wavelength range from 5500 to 9000  $\text{cm}^{-1}$  are used, the model can be built even by using a very small band of 50 variables no matter the strong absorption peak (around 6900  $\text{cm}^{-1}$ ) of O–H or N–H is used or not.

### 3.2. Quantitative determination of composition

The establishment of QSTR model is exciting because it provide a new way to predict temperature of mixture solutions. The quan-

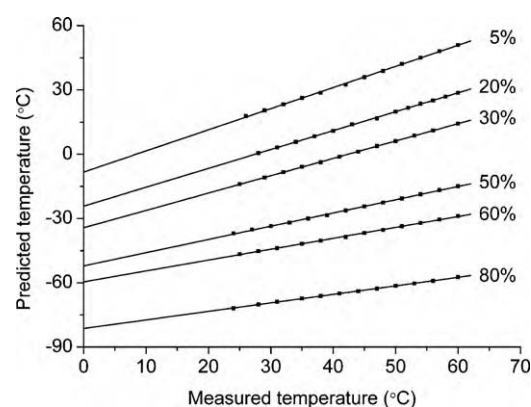


Fig. 3. Relationship of the measured temperature and predicted results of aqueous ethanol solutions by using the QSTR model of water.

titative determination of composition, however, is more attractive. Theoretically, the composition of a sample should have effects on the spectrum, though no significant difference can be found, and the effects should be reflected in the QSTR model. The difference between the models of different solutions may be employed for investigation of concentration. Therefore, the relationship of measured temperature and the predicted one for a mixture solution by using the model of the solvent was investigated.

Aqueous ethanol solutions with different concentration were examined at first, i.e., the temperature of aqueous ethanol solutions was predicted by the QSTR model of pure water. The relationship between the measured and predicted temperature for the six solutions with the ethanol concentration from 5% to 80% (v/v) is shown in Fig. 3. Inspiringly, there is a very good linearity between the measured and predicted temperature for the solutions of each concentration. However, large deviations in the intercept can be found, which may be ascribed to the interaction between water and ethanol. It should be noted that, in the calculation, the wavelength region 6136–5496  $\text{cm}^{-1}$ , which does not contain the strong absorption peak of water, was used, possibly because the existence of the strong peak may mask the small difference between the NIR spectra.

Examining the variation of the deviation with concentration in Fig. 3, it can be found that the deviation gets larger with the increase of ethanol concentration. Therefore, the variation of intercept with the concentration was plotted in Fig. 4 and the regression equation of the curve was displayed in the first line of Table 3. It can be clearly seen that the intercept in Fig. 3 has a nearly linear decrease with the increase of ethanol concentration. The correlation coefficient (*R*), which is obtained by linear regression, is 0.9993, indicating that the variation of intercept is correlative very well with ethanol concentration. Therefore, the curve in Fig. 4 can be used as calibration curve for quantitative determination of the ethanol concentration in the water–ethanol mixture.

Table 2  
PLS models for predicting temperature and the results of cross validation.

Sample	Temperature range/°C	Number of data points	Number of latent variables	<i>R</i>	RMSECV
Water	24–60	12	4	0.9998	0.1739
Ethanol	24–60	13	3	0.9999	0.1891
<i>n</i> -hexane	28–60	11	3	0.9996	0.2971
Water–ethanol	24–60	13	3	0.9997	0.2806
Ethanol– <i>n</i> -hexane	24–59	12	3	0.9999	0.1352
Water–ethylenediamine	25–60	12	3	0.9999	0.1423
Ethanol–ethylenediamine	25–60	12	3	0.9999	0.1554
Water–methanol–ethanol	26–60	12	3	0.9999	0.1086
Water–ethanol–ethylenediamine	26–60	12	3	0.9999	0.1797

**Table 3**  
Calibration curves established with the intercepts in the relationship of predicted and measured temperature.

Solvent	Solute	Wavelength regions/cm <sup>-1</sup>	Calibration curve <sup>a</sup>	R
Water	Ethanol	6136–5496	$y = -4.52 - 0.95x$	0.9993
Ethanol	Ethylenediamine	6981–5496	$y = -28.19 + 14.70x$	0.9989
Water–ethanol (1:1, v/v)	Ethylenediamine	7367–5496	$y = -5.65 - 0.41x$	0.9993
Water	Ethanol (25% methanol)	6316–5496	$y = -55.71 - 2.29x$	0.9994

<sup>a</sup>  $y$  is the intercept and  $x$  the concentration (% v/v).

For further investigation of the calibration curve, the mixtures of ethanol and ethylenediamine were studied in the same way as above, i.e., the temperature of the mixture was predicted by using the model of ethanol, and the concentration of ethylenediamine was the target of calibration. The results are summarized in the second line of Table 3. Furthermore, mixtures composed of three components were also investigated. The third line of Table 3 lists the results for the mixtures of water, ethanol and ethylenediamine. In the calculation, the QSTR model of water–ethanol (1:1, v/v) was used and the target of calibration was ethylenediamine. The fourth line of Table 3 shows the results for the mixtures of water, methanol and ethanol, in which 25% (v/v) methanol is contained as an interference composition. In the calculation, the QSTR model of water was used and the target of calibration was ethanol. The same thing that needs to be noted is that different wavelength regions were used in the calculations, as listed in the table. Clearly, the same results as above were obtained. The variation of the intercept changes almost linearly with the concentration of the calibration target. From these results, it can be concluded that quantitative determination of the composition in a mixture can be achieved by using the difference between QSTR models, i.e., the intercept in the relationship between the measured and predicted temperature of the mixture.

### 3.3. Validation of the calibration curves

In order to investigate the feasibility of the calibration curves in quantitative determination, external validation is further performed with two aqueous ethanol solutions and a Chinese alcohol liquor sample. The concentration of the two solutions were prepared to be 10% (v/v) and 70% (v/v), which lie in the range of the calibration curve (5–80%, v/v), and the reference concentration of the alcohol liquor sample was obtained by gas chromatography. In the validation, the same conditions as above for measuring the NIR spectra were used, but the spectra were measured at 12 different temperatures from 25 to 60 °C, respectively. It is worthy of note that the data points number for the spectra must be exactly same as that

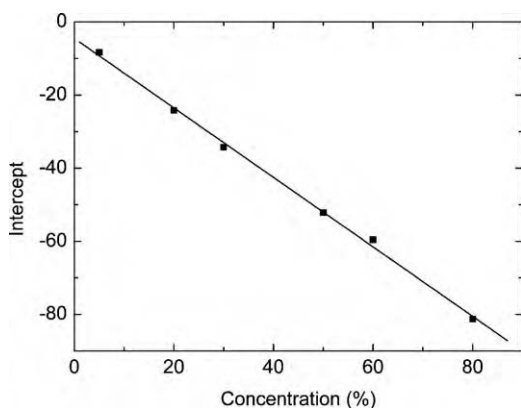


**Fig. 4.** Calibration curve for ethanol concentration in aqueous ethanol solutions established with intercepts in the relationship of the measured temperature and predicted results.

**Table 4**  
Analytical results of validation samples.

No.	Sample	Reference (%)	Predicted (%)	Recovery (%)
1	Water–ethanol mixture	10.00	9.61	96.1
2	Water–ethanol mixture	70.00	70.13	100.2
3	Alcohol liquor	35.62 (0.72) <sup>a</sup>	36.16	101.5

<sup>a</sup> The concentration was measured by gas chromatography. The number is the mean of three measurements, and the number in the parentheses is the standard deviation. The concentration labeled is 38 (% v/v).

used in building the QSTR model, but different temperatures can be used to measure the spectra. Because all of the samples were mixture of water and ethanol, the QSTR model of pure water as shown in Fig. 2 was adopted for temperature prediction, and the calibration curve displayed in Fig. 4 was used for quantitative determination. The results are listed in Table 4. It can be found that the recoveries of ethanol were between 96.1% and 101.5%.

## 4. Conclusion

The properties of the temperature dependent NIR spectra were quantitatively studied. Based on the NIR spectra of the commonly used solvent (water, *n*-hexane, methanol and ethanol) and ethylenediamine measured at different temperature from 25 to 60 °C, QSTR models were built by using PLS regression, and calibration curves for quantitative determination of the composition of mixtures were also established by using the difference between the models. The correlation coefficients between the measured and predicted temperature were found to be as high as above 0.99 for the QSTR model, and calibration curves obtained with the variation of concentration with the deviation between the measured and predicted temperature were also found to be reliable. The QSTR model can be used for prediction of temperature and the calibration curves can be employed for quantitative determination of the composition in mixtures by using NIR spectroscopic technique. However, only the samples of two or three components were investigated and the method was validated with only one real sample in this study. On the other hand, there are still limitations for practical uses of the method for quantitative determination, because spectra at several temperatures must be measured. Therefore, further studies are still needed to validate the practicability for real samples and to prove the universality of the method.

## Acknowledgement

This study is supported by National Natural Science Foundation of China (No. 20835002).

## References

- [1] M.A. Czarnecki, Y. Liu, Y. Ozaki, M. Suzuki, M. Iwahashi, Appl. Spectrosc. 47 (1993) 2162–2168.
- [2] D. Wojtkow, M.A. Czarnecki, J. Phys. Chem. A 110 (2006) 10552–10557.
- [3] I. Noda, Y. Liu, Y. Ozaki, J. Phys. Chem. 100 (1996) 8674–8680.
- [4] J.R. Collins, Phys. Rev. 26 (1925) 771–779.
- [5] W.C. Waggener, Anal. Chem. 30 (1958) 1569–1570.
- [6] W.A.P. Luck, Ber. Bunsenges. Phys. Chem. 69 (1965) 626–637.
- [7] J. Lin, C.W. Brown, Appl. Spectrosc. 47 (1993) 1720–1727.

- [8] V.S. Langford, A.J. McKinley, T.I. Quickenden, *J. Phys. Chem. A* 105 (2001) 8916–8921.
- [9] R. Oder, D.A.I. Goring, *Can. J. Chem.* 48 (1970) 3790–3796.
- [10] S.R. Delwiche, K.H. Norris, R.E. Pitt, *Appl. Spectrosc.* 46 (1992) 782–789.
- [11] P.S. Jensen, J. Bak, S. Andersson-Engels, *Appl. Spectrosc.* 57 (2003) 28–36.
- [12] M.A. Czarnecki, K.Z. Haufa, *J. Phys. Chem. A* 109 (2005) 1015–1021.
- [13] M.A. Czarnecki, D. Wojtkow, *J. Phys. Chem. A* 108 (2004) 2411–2417.
- [14] Y. Ozaki, Y. Liu, I. Noda, *Macromolecules* 30 (1997) 2391–2399.
- [15] P.Y. Wu, Y.L. Yang, H.W. Siesler, *Polymer* 42 (2001) 10181–10186.
- [16] Y. Liu, Y. Ozaki, I. Noda, *J. Phys. Chem.* 100 (1996) 7326–7332.
- [17] S. Sasic, V.H. Segtnan, Y. Ozaki, *J. Phys. Chem. A* 106 (2002) 760–766.
- [18] I. Noda, *J. Am. Chem. Soc.* 111 (1989) 8116–8118.
- [19] I. Noda, Y. Liu, Y. Ozaki, *J. Phys. Chem.* 100 (1996) 8665–8673.
- [20] I. Noda, Y. Liu, Y. Ozaki, M.A. Czarnecki, *J. Phys. Chem.* 99 (1995) 3068–3073.
- [21] F.O. Libnau, J. Toft, A.A. Christy, O.M. Kvalheim, *J. Am. Chem. Soc.* 116 (1994) 8311–8316.
- [22] B. Czarnik-Matusiewicz, S. Pilorz, *Vib. Spectrosc.* 40 (2006) 235–245.
- [23] V.H. Segtnan, S. Sasic, T. Isaksson, Y. Ozaki, *Anal. Chem.* 73 (2001) 3153–3161.
- [24] B. Jaillais, R. Pinto, A.S. Barros, D.N. Rutledge, *Vib. Spectrosc.* 39 (2005) 50–58.
- [25] F. Wulfert, W.T. Kok, A.K. Smilde, *Anal. Chem.* 70 (1998) 1761–1767.
- [26] M. Blanco, D. Valdes, *J. Near Infrared Spectrosc.* 2 (2004) 121–126.
- [27] Y. Wang, B.R. Kowalski, *Anal. Chem.* 65 (1993) 1301–1303.
- [28] K. DeBraekeleer, F. Cuesta Sanchez, P.A. Hailey, D.C.A. Sharp, A.J. Pettman, D.L. Massart, *J. Pharm. Biomed. Anal.* 17 (1998) 141–152.
- [29] F. Wulfert, W.T. Kok, O.E. de Noord, A.K. Smilde, *Anal. Chem.* 72 (2000) 1639–1644.
- [30] K.H. Hazen, M.A. Arnold, G.W. Small, *Appl. Spectrosc.* 48 (1994) 477–483.
- [31] S.Y.B. Hu, M.A. Arnold, J.M. Wiencek, *Anal. Chem.* 72 (2000) 696–702.
- [32] A. Lorber, *Anal. Chem.* 58 (1986) 1167–1172.
- [33] J.T. Olesberg, M.A. Arnold, S.Y.B. Hu, J.M. Wiencek, *Anal. Chem.* 72 (2000) 4985–4990.
- [34] A.C. Peinado, F. van den Berg, M. Blanco, R. Bro, *Chemom. Intell. Lab. Syst.* 83 (2006) 75–82.
- [35] D.M. Haaland, E.V. Thomas, *Anal. Chem.* 60 (1988) 1193–1202.